

Faraday Discussions

Accepted Manuscript



This manuscript will be presented and discussed at a forthcoming Faraday Discussion meeting. All delegates can contribute to the discussion which will be included in the final volume.

Register now to attend! Full details of all upcoming meetings: <http://rsc.li/fd-upcoming-meetings>



This is an *Accepted Manuscript*, which has been through the Royal Society of Chemistry peer review process and has been accepted for publication.

Accepted Manuscripts are published online shortly after acceptance, before technical editing, formatting and proof reading. Using this free service, authors can make their results available to the community, in citable form, before we publish the edited article. We will replace this *Accepted Manuscript* with the edited and formatted *Advance Article* as soon as it is available.

You can find more information about *Accepted Manuscripts* in the [Information for Authors](#).

Please note that technical editing may introduce minor changes to the text and/or graphics, which may alter content. The journal's standard [Terms & Conditions](#) and the [Ethical guidelines](#) still apply. In no event shall the Royal Society of Chemistry be held responsible for any errors or omissions in this *Accepted Manuscript* or any consequences arising from the use of any information it contains.

Cite this: DOI: 10.1039/c0xx00000x

www.rsc.org/xxxxxx

ARTICLE TYPE

Aptamer-Conjugated Theranostic Hybrid Graphene Oxide with Highly Selective Biosensing and Combined Therapy Capability

Bhanu Priya Viraka Nellore, Avijit Pramanik, Suhash Reddy Chavva, Sudarson Sekhar Sinha, Christen Robinson, Zhen Fan, Rajashekhar Kanchanapally, Justin Grennell, Ivy Weaver, Ashton T. Hamme and Paresh Chandra Ray *

Received (in XXX, XXX) Xth XXXXXXXXXX 20XX, Accepted Xth XXXXXXXXXX 20XX

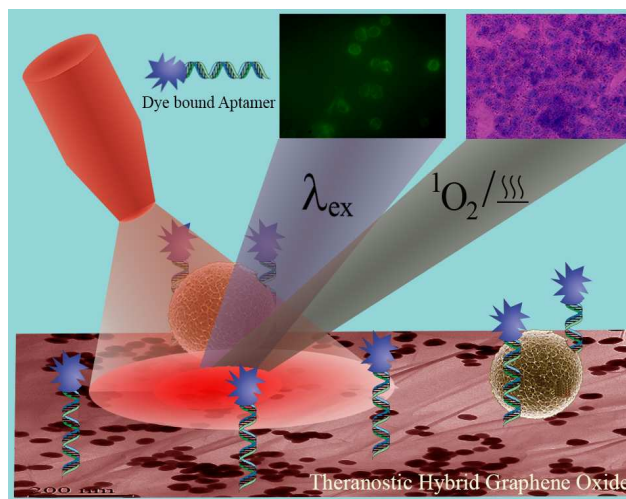
DOI: 10.1039/b000000x

Cancer is one of the life-threatening diseases which is rapidly becoming a global pandemic. Driven by the need, here we report for the first time aptamer conjugated theranostic magnetic hybrid graphene oxide based assay for highly sensitive tumor cell detection from blood sample with combined therapy capability. AGE-aptamer conjugated theranostic magnetic nanoparticle attached hybrid graphene oxide was developed for highly selective detection of tumor cells from infected blood sample. Experimental data indicate that hybrid graphene can be used as multi-color luminescence platform for selective imaging of G361 human malignant melanoma cancer cells. Reported results have also shown that indocyanine green (ICG) bound AGE-aptamer attached hybrid graphene oxide is capable of combined synergistic photothermal & photodynamic treatment of cancer. Targeted combined therapeutic treatment using 785 nm NIR light indicates that the multimodal therapeutic treatment is highly effective for malignant melanoma cancer therapy. Reported data show that aptamer conjugated theranostic graphene oxide based assay has exciting potential for improving cancer diagnosis and treatment.

Introduction

Cancer is known for more than three thousand years, but till in 21st century, it is one of the most life-threatening diseases, causes 1 in 8 deaths worldwide¹⁻⁵. With advances on our understanding of the signaling pathways, now we realize that the detection of circulating tumor cells (CTCs) could be an invaluable tool for the early stage detection of cancer and for monitoring the progression⁴⁻¹⁰. Malignant melanoma is the most deadly human skin cancer, which is responsible for 75.2% of skin cancer-related deaths. Malignant melanoma cell line G361 is aggressive form of skin cancer that is highly resistant to conventional therapies and known to be resistant to apoptosis¹⁻⁵. As a result, simple blood test for the finding of circulating G361 melanoma cells can help to identify if melanoma has spread to other areas of the body.

^a Department of Chemistry and Biochemistry, Jackson State University, Jackson, MS, USA; E-mail:paresh.c.ray@jsums.edu; Fax:+16019793674



Scheme 1: Schematic representation showing aptamer bound theranostic magnetic nanoparticle attached hybrid graphene oxide with targeted separation, diagnostic and combined synergistic treatment capability of malignant melanoma cancer cells.

Since CTCs are the very few rare malignant cells in blood containing several millions of red blood cells, extremely sensitive and specific methods are required to detect early stage CTCs⁸⁻¹⁷. In the last decade, due to the remarkable electronic and structural properties, graphene has revolutionized the scientific community¹⁹⁻³⁸. However, the development of graphene-based material for selective CTC detection and therapy is still in its infancy³⁹⁻⁴¹. This requires graphene with novel functionality which has selective bio-sensing and therapy capability. Driven by the need, here we report that aptamer conjugated theranostic graphene oxide based assay has exciting potential for improving cancer diagnosis by detecting CTC from infected blood. Recently, several articles have demonstrated that photoluminescence of graphene can be observed by modifying with various oxygen-containing groups or by reducing its size to the nanometer scale³⁰⁻³³. By using the wonderful tunable fluorescence properties of graphene oxide (GO), here we demonstrate that hybrid graphene can be used as multi-color luminescence platform for selective

imaging of G361 human malignant melanoma cancer cells, as shown in Scheme 1. Since AGE-aptamer is known to be selective for G361 human malignant melanoma cancer cells⁵, we have used AGE-aptamer attached hybrid graphene oxide for selective imaging of malignant melanoma cancer cells. Our reported results also show that the multimodal therapeutic action using ICG-bound hybrid graphene oxide is highly promising for malignant melanoma cancer therapy.

Molecular underpinnings of cancer drug resistance has advanced significantly¹⁰⁻¹⁷. We now understand that a single therapeutic agent can have limited efficiencies in clinical environment due to the drug-resistance profiles¹⁰⁻¹⁷. As a result, multimodal therapy holds highly promising strategy with minimum side effects¹⁰⁻¹⁷. Design of theranostic hybrid graphene oxide for selective diagnostic and therapeutic cancer therapy can have revolutionary impact on the pharmaceutical industry²⁴⁻³⁰. In the last decade, several different types of nanoparticle based therapeutic approaches have been developed for possible cancer treatment¹⁻⁹. Among all these, near infrared light driven photothermal therapy (PTT) and photodynamic therapy (PDT) have been shown to possess unique advantages, including remote controllability, low systemic toxicity and side effects^{5-15,34-37}. Since the combination of therapeutic approaches may cooperatively suppress cancer development^{10,34-37}, here we report the indocyanine green (ICG) bound magnetic nanoparticle attached graphene oxide platform for combined photodynamic and photothermal synergistic targeted therapy of cancer, as shown in Scheme 1. ICG is a water-soluble photosensitizer approved by the U.S. Food and Drug Administration (FDA)³⁴⁻³⁷. Experimental data demonstrated that due to the synergistic effect, the therapeutic efficacy of nano-platform was enhanced significantly compared to PDT or PTT alone.

Experimental

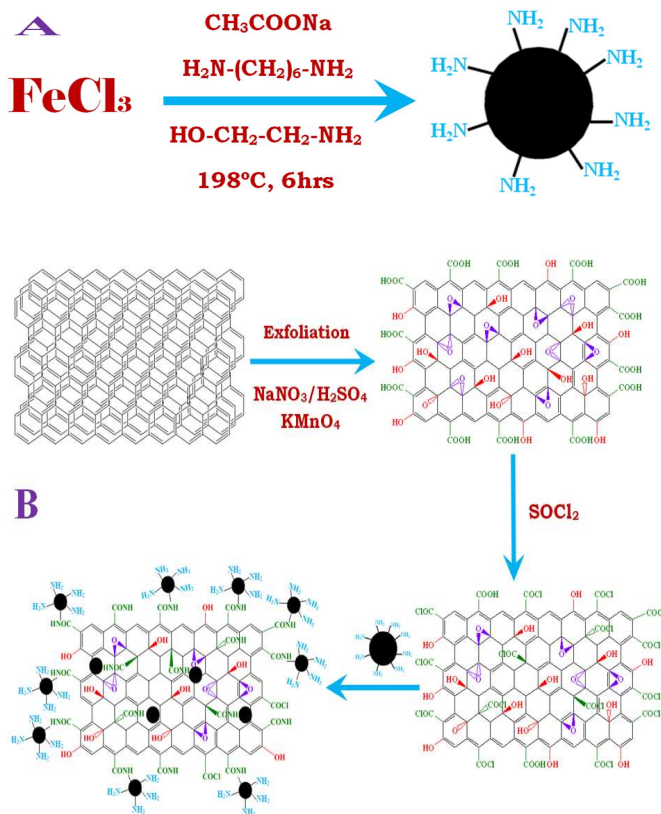
All chemicals, including graphite, KMnO_4 , sodium borohydride, iron chloride, sodium citrate, were purchased from Sigma-Aldrich and Fisher Scientific. We have obtained G361 melanoma cells, growth media to grow cancer cells, buffered saline, trypsin, and fetal bovine serum from the American Type Culture Collection (ATCC, Rockville, MD).

Preparation of Amine functionalized magnetic nanoparticles

The magnetic nanoparticles were prepared using two-step processes as shown in Scheme 2A. For this purpose, in the first step we have dissolved FeCl_3 (1.0g) in ethylene glycol (30mL). In next step, anhydrous sodium acetate (2.0g) and 1,6-hexadamine (6.5g) were added and stirred vigorously to acquire a transparent solution. The mixture was sealed in a Teflon-lined stainless steel autoclave and was heated at 198 °C for 6 h. The product washed with hot water and ethanol (3 times) under ultrasonic condition using a magnet to remove the solvent and unbound 1,6-hexadamine effectively, and then dried at 50 °C to gain the black powder. Magnetic nanoparticles were characterized using JEM-2100F transmission electron microscope (TEM) as shown Figure 1A, which shows that the average particle size is about 40 nm. Magnetic properties were determined using a superconducting quantum interference device (SQUID) magnetometer at room temperature, which indicates super-paramagnetic behavior with specific saturation magnetization of 43.5 emu g^{-1} for the amine-functionalized magnetite nanoparticles.

Preparation of magnetic nanoparticle attached hybrid graphene oxide

Magnetic nanoparticle attached graphene oxide was synthesized using several step processes as shown in Scheme 2B. At first, graphene oxide was prepared from graphite. For this purpose, we have used modified Hummers reported method³⁸ for graphite exfoliation.



Scheme 2: A) Schematic representation showing our synthesis procedure to develop magnetic nanoparticle. B) Schematic representation showing our synthesis procedure to develop magnetic nanoparticle attached hybrid graphene oxide.

We have used strong oxidizing agents to yield graphene oxide as shown in Scheme 1B. For this purpose, 1g of graphite powder was added to 1g of NaNO_3 in 45 mL of H_2SO_4 , under stirring in an ice bath. Then 3g of KMnO_4 added very carefully, to not to increase the temperature. Next, we have transferred the reaction mixture container to a water bath, which is at 35°C and stirred it for 30 minutes. A thick paste was obtained. After that, 45 mL of water was added drop wise very carefully. During the addition of water, temperature raised to around 95 to 98°C . Then we have added 140 mL of water and kept the mixture for 30 more minutes. Next, we have performed filtration and re-dispersed the obtained graphene oxide in 100 mL of water. After that, we have performed sonication for 1 hour for exfoliation. After that, we have characterized water soluble graphene oxide using IR and Raman spectroscopy, as we have reported recently.

In the next step, for the attachment of amino-functionalized magnetic nanoparticle with graphene oxide, acid chloride functionalized graphene oxide were prepared. For this purpose, $-\text{COOH}$ functionalized graphene oxide was treated with thionyl chloride in the presence of dimethylformamide catalyst. As

shown in the Scheme 1B, the acid chloride group was used as a chemical anchor for the connection with amine functionalized magnetic nanoparticles. Transmission electron microscopy (TEM, JEM-2100F instrument) data, as shown in Figure 1B, clearly indicate that in hybrid graphene oxide, magnetic nanoparticles are attached onto graphene oxide. Size of magnetic nanoparticle in hybrid graphene oxide is about 40 nm. From Figures 1A and 1B, we can clearly see that the size and shape of magnetic nanoparticle remain the same after conjugation, which indicates that the morphology of magnetic nanoparticle remains unchanged during coupling between graphene oxide and magnetic nanoparticle. Our experimental data also indicate that magnetic nanoparticle agglomeration is much lower when nanoparticles are attached with graphene oxide, which will be useful for bio-medical applications. Figure 1D indicates that our hybrid graphene oxide is highly magnetic, and as a result, we can separate them by using a small bar magnet. superconducting quantum interference device (SQUID) measurement indicates that hybrid graphene oxide exhibits super-paramagnetic behavior with specific saturation magnetization 26.4 emu g^{-1} . Figure 1C shows the Raman spectrum of hybrid graphene oxide, which displays a D-band at 1340 cm^{-1} and a G-band at 1612 cm^{-1} . In the reported spectra, the strong D band clearly indicates that the degree of oxidation is high. To understand the amount of magnetic nanoparticle in the hybrid graphene oxide, we have used thermogravimetric analysis (TGA), using Perkin-Elmer thermogravimetric analyzer. From the TGA data we have estimated that the mass fraction of magnetic nanoparticle and graphene oxides are about 30 and 70 wt %, respectively.

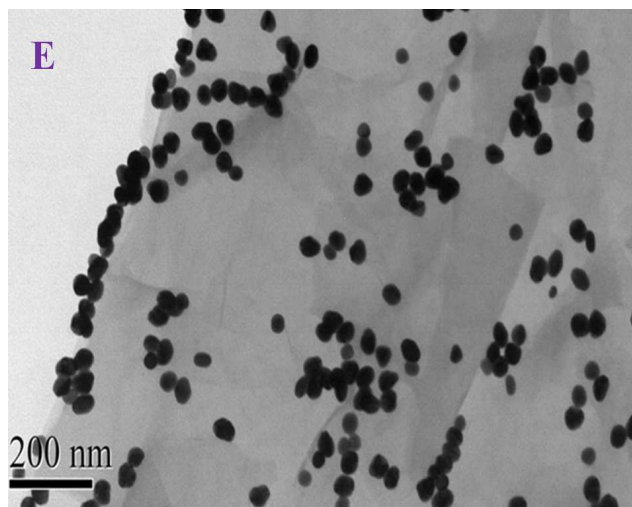
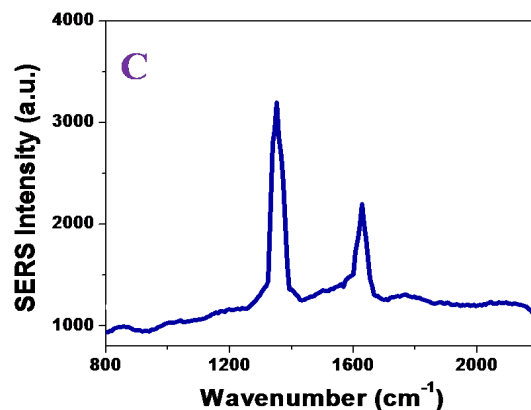
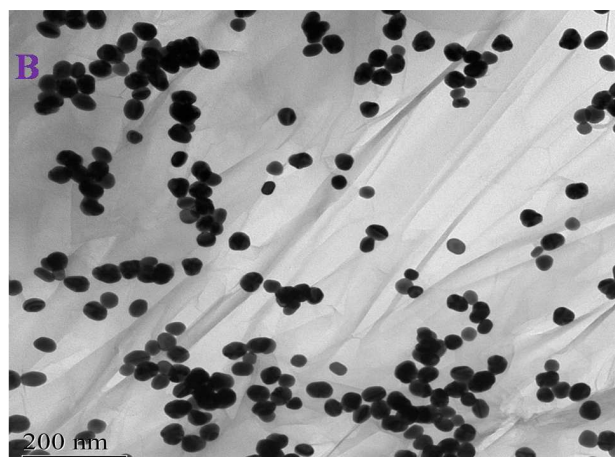
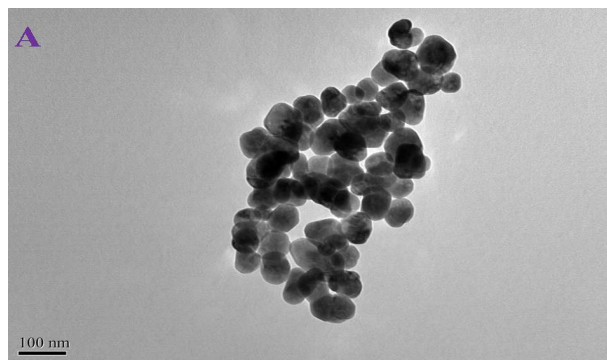


Figure 1: A) TEM picture shows the morphology of freshly prepared magnetic nanoparticle. B) TEM picture shows the morphology of freshly prepared magnetic nanoparticle attached hybrid graphene oxide. C) Raman spectra showing graphene oxide D-band at $\sim 1340 \text{ cm}^{-1}$ and G-band at $\sim 1612 \text{ cm}^{-1}$ in hybrid material. D) Photograph shows that the magnetic nanoparticle attached hybrid graphene oxide is highly magnetic, and as a result, we can separate them by using a bar magnet. E) TEM picture shows the morphology of freshly prepared aptamer bound magnetic nanoparticle attached hybrid graphene oxide

Preparation of aptamer-conjugated hybrid graphene oxide

For targeted imaging of malignant melanoma G361 cells and synergistic therapy, we have modified nanoplateform with MB-bound AGE- aptamer, which is known to be specific to malignant melanoma G361 cells. For this purpose, initially, hybrid graphene oxide was coated by thiolated polyethylene glycol (HS- PEG),

which helps to avoid nonspecific interactions with cells and cell media. After PEGylation, NH-modified AGE- aptamers were attached with acid chloride functionalized graphene oxide. As shown in Figure 1E, TEM data clearly indicate that in aptamer bound hybrid graphene oxide, magnetic nanoparticles are attached onto graphene oxide. From the TEM data reported at 1B and 1E, we clearly see that the morphology looks similar, which indicate that during aptamer bounding process, the morphology remains the same for hybrid graphene oxide.

Cell culture and incubation with hybrid graphene oxide

Malignant melanoma G361 cells were grown according to the ATCC procedure. We have grown cells in a 5% CO₂ incubator at 37°C using RPMI-1640 medium (ATCC, Rockville, MD) supplemented with 10% premium fetal bovine serum (FBS) (Lonza, Walkersville, MD) and antibiotics (10 IU/mL penicillin G and streptomycin) in 75-cm² tissue culture flasks. Once we have a culture of 10⁵ cells/mL, different numbers of malignant melanoma G361 cells were spiked in citrated whole rabbit blood at various densities. After that, different concentrations of magnetic- hybrid graphene oxide were mixed with infected blood for 30 minutes at room temperature before performing the magnetic separation experiment. After magnetic separation, we performed TEM and fluorescence analyses.

Fluorescence analysis

After malignant melanoma G361 cells separation by the magnet, we used an Olympus IX71 inverted confocal fluorescence microscope fitted with a SPOT Insight digital camera for fluorescence imaging.

Combined destruction of malignant melanoma G361 cells and determination of the percentage of live cells

For the PDT, PTT or combined destruction experiments, we have used a continuous-wavelength OEM laser operating at 785 nm at 2 W/cm² power for 10–25 minutes. For finding the amount of cell death, we have used MTT (ATCC CA# 30-1010k) and typan blue test, using our reported method⁹⁻¹⁰.

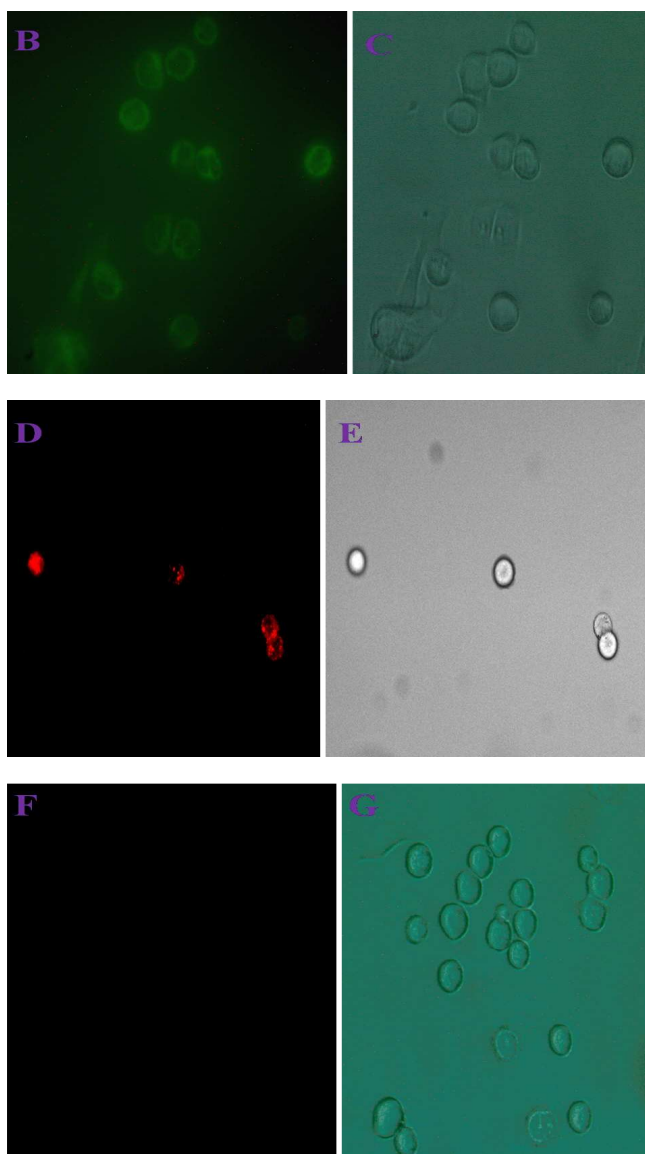
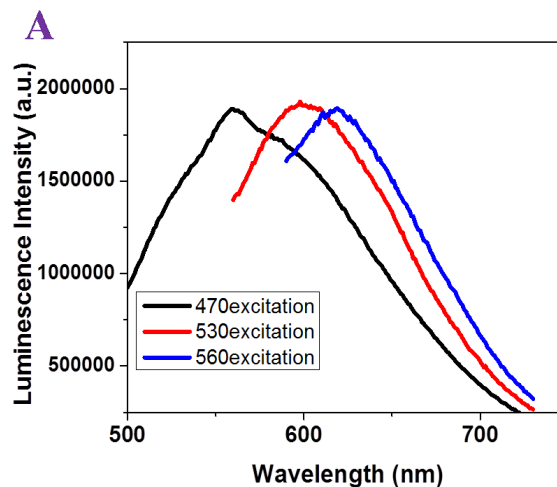
ROS generation measurement

To understand how ROS formation varies with PTT, we have measured the amount of reactive oxygen species formed during PDT and combined therapy process. For this purpose, we have used singlet oxygen sensor green reagent (SOSG, Sigma) and followed manufacturer's protocol. For fluorescence measurement, we have used 485 nm light as excitation source and the fluorescence intensity was measured at 528 nm using the microplate reader.

Results and Discussions

Our label-free cancer cell imaging using aptamer-conjugated hybrid graphene oxide is based on the graphene oxide luminescence properties. As shown in Figure 2A, the fluorescence properties of magnetic-graphene oxide can be tuned just by varying the excitation energy without changing its chemical composition and size. Our observed excitation energy dependent photoluminescence spectral shift for hybrid graphene oxide can be due to the several factors³⁰⁻³³ and these are as follows: 1) excitation wavelength dependent fluorescence from

65 the –OH moiety in the graphene oxide sheets; 2) Due to the local reorganization of photoexcited GO sheets in a polar solvent, the solvent relaxation time becomes comparable to the fluorescence lifetime.



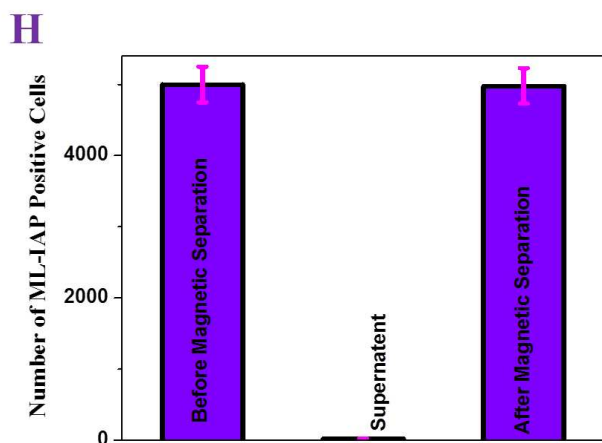


Figure 2: A) Excitation wavelength dependent photoluminescence from freshly prepared magnetic nanoparticle attached hybrid graphene oxide. Plot clearly shows that photoluminescence can be tuned just by varying the excitation energy, without changing the size. B) Fluorescent images of aptamer conjugated hybrid graphene oxide attached G361 human malignant melanoma cancer cell after separation from blood sample using a magnet. We have used 470 nm light as excitation source. C) Bright-field image of the same cells after magnetic separation. D) Fluorescence image of aptamer conjugated hybrid graphene oxide attached G361 human malignant melanoma cancer cell, after separation from blood sample using a magnet. We have used 560 nm light as an excitation source. E) Bright-field image of the same cells after magnetic separation, F) Fluorescence image of supernatant after magnet separation. Our result clearly shows that aptamer attached hybrid graphene oxide does not bind with blood cells. G) Bright-field image of same supernatant after magnetic separation. H) Number of ML-IAP positive cells before and after magnetic separation, measured by immunosorbent assay.

To understand whether aptamer conjugated hybrid graphene oxide developed by us can be used for G361 human malignant melanoma cancer cell analysis from the blood sample in the settings close to clinical diagnosis, G361 malignant melanoma cancer cells were spiked at various densities into the suspensions of citrated whole rabbit blood. After 80 minutes of gentle shaking, we incubated 150 μ L aptamer-conjugated hybrid magnetic graphene oxide with 2.5 mL of G361 malignant melanoma cells infected blood sample. Next, we have incubated the mixture for 40 minutes at room temperature under gentle shaking. After that, we have used a bar magnet to separate & enrich malignant melanoma G361 cells attached with hybrid magnetic graphene oxide. Next, the supernatant blood sample was carefully removed with a pipette. After that, the suspensions of the magnetic graphene oxide attached G361 malignant melanoma cells and supernatant were characterized using TEM, fluorescence imaging and enzyme-linked immunosorbent assay (ELISA) analysis kits, as shown in Figure 2. The melanoma inhibitor of apoptosis protein (ML-IAP) is well known to over express in malignant melanoma cell, which is known to help in disease progression and treatment resistance. As shown in Figure 2H, our enzyme-linked immunosorbent assay results reveal that no ML-IAP presence in the fractions of cell suspensions that did not bind to aptamer conjugated magnetic graphene oxide, which indicates the absence of malignant melanoma G361 cells in cell suspension which are not separated by the magnet. So, they are mainly blood cells. On the other

hand, we find that ML-IAP was present in the magnetic graphene oxide attached cell suspension. Enzyme-linked immunosorbent assays result, as shown in Figure 2H, clearly indicates that malignant melanoma G361 cells are attached with nanoplateform. From the enzyme-linked immunosorbent assay experiments we have estimated that the malignant melanoma G361 cell recovery by the bar magnet was about 97%.

Figure 2A-2G shows confocal fluorescence microscope imaging data, which clearly indicate that aptamer conjugated graphene oxide can be used for label-free imaging of cancer cells. To understand whether the luminescence of graphene oxide can be tuned for multicolor cancer imaging, we have performed fluorescence imaging experiment using 470 nm and 560 nm excitation. Figure 2B and 2D clearly show that the luminescence of graphene oxide can be used for multi-color cancer imaging and it is due to the fact that single-photon photoluminescence from graphene oxide can be tuned, just by varying the excitation energy without changing its chemical composition and size, as we have discussed before. As shown in Figure 2E, no fluorescence was observed from the cell suspension which are not separated by the magnet and it due to the fact that malignant melanoma G361 cells are absent in cell suspension which are not separated by the magnet. Our fluorescence imaging results also indicate that our hybrid magnetic graphene oxide can be used to separate malignant melanoma G361 cells from the blood sample in clinical environment. Similarly, TEM image, as shown in Figure 3A, shows magnetic graphene oxide attached malignant melanoma G361 cells. All the experimental results described above clearly show that aptamer-conjugated hybrid magnetic graphene oxide developed by us is highly selective for binding with the malignant melanoma G361 cell line and can be used for selective detection of malignant melanoma from blood sample.

After successful targeted malignant melanoma G361 cells separation, we have performed NIR light driving therapy experiments using 785nm excitation light. Before therapy experiment, to understand the cytotoxicity of hybrid graphene oxide in the absence of NIR light, hybrid graphene oxide attached G361 cells were incubated for 12 hours without any laser light. Our experimental data, as shown in Figure 3D, clearly show that no cell death was observed even after 12 hours of incubation, which indicates that hybrid graphene oxide developed by us is not cytotoxic in the absence of external NIR light. Next, we have performed 785 nm light driven photothermal therapy experiment. To determine the amount of cell death due to the hybrid graphene oxide hypothermia effect, we added trypan blue after NIR radiation exposure. Since living cells cannot bind with trypan blue, they were colorless. On the other hand, dead cells bind with the blue dye and became blue. Therefore, cell viability can be qualitatively determined from the color of the cell monolayer. As shown in Figure 3B, some of the cancer cells were dead after 20 min of the PTT process. Using MTT test, we have find out that 23% cancer cells were dead due to the PTT, as shown in Figure 3D, when hybrid graphene oxide attached G361 cells were irradiated with 785 nm light at 1 W/cm² power for 20 minutes. Since graphene oxide absorbed 785 nm light and converted it into heat through nonradiative decay, G361 malignant melanoma cells were killed in the presence of 785 nm NIR light, which is mainly due to the hypothermia. Since graphene oxide absorption cross-section is very low at 785 nm, the observed hypothermia effect is also low.

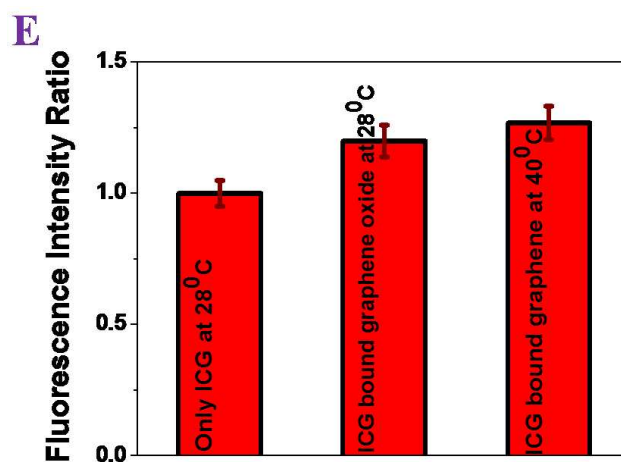
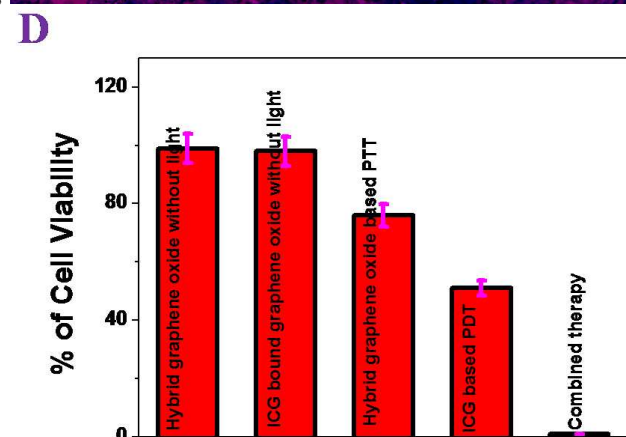
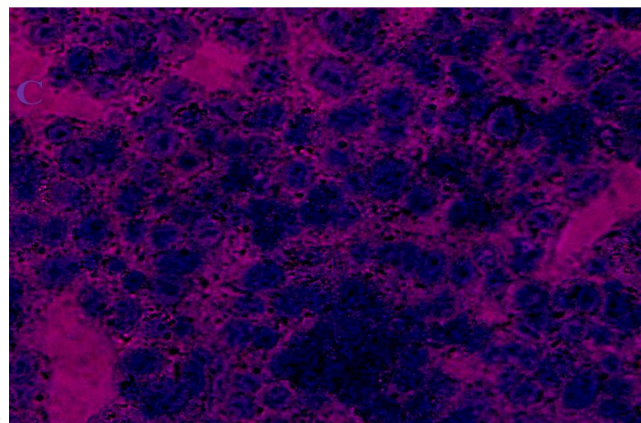
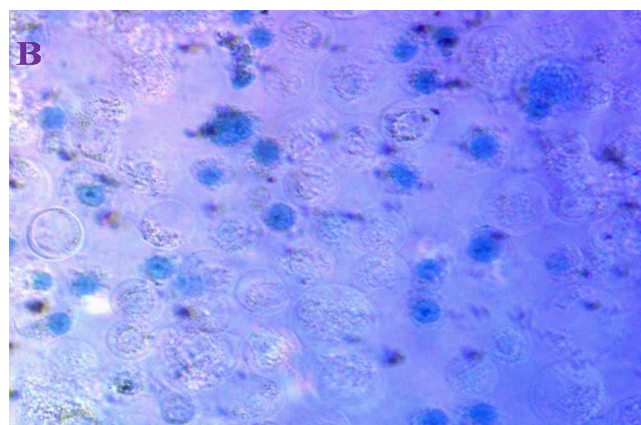
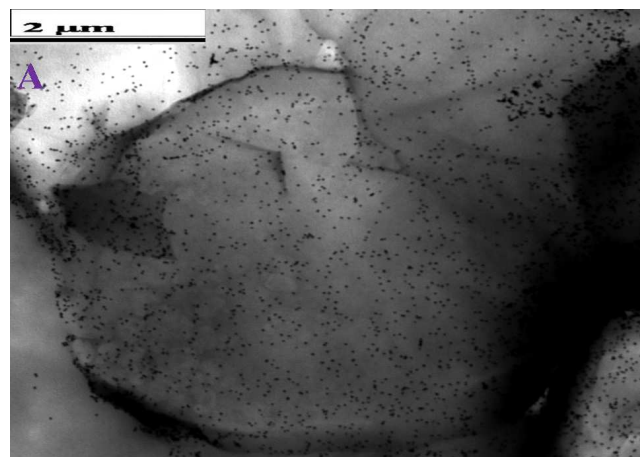


Figure 3: A) TEM image shows malignant melanoma G361 cells inside the aptamer conjugated magnetic graphene oxide sheet after magnetic separation. B) Bright-field inverted microscopic images of hybrid graphene oxide attached malignant melanoma G361 cells, after separation by a magnet and followed by irradiation with 785 nm near IR light at 1 W/cm² for 20 minutes. For imaging, we have used 485 nm excitation and the fluorescence has been collected between 520-535 nm. Bright field image clearly shows that some cancer cells are dead after PTT. C) Bright-field inverted microscopic images of ICG bound hybrid graphene oxide attached malignant melanoma G361 cells after separation by a magnet and followed by irradiation with 785 nm near IR light at 1 W/cm² for 20 minutes. Bright field image clearly shows that most cancer cells are dead after combined therapy. D) Plot showing the percentage of cell viability in ICG-bound hybrid graphene oxide attached malignant melanoma G361 cells in the absence of laser light. It also shows how the cell viability varies in the presence of laser light. Plot shows no cytotoxicity in the absence of NIR light. It also shows dramatic synergistic action in case of combined therapy. E) Plot showing how ROS formation from ICG can vary in the presence of hybrid graphene oxide at different temperatures.

30

To improve the NIR light driving cancer cell killing efficiency, we have synthesized Indocyanine green (ICG) bound AGE-aptamer attached hybrid graphene oxide as combined therapy material. Next, to find out whether the combined therapy is much superior to single therapy, we have performed several different experiments which we will discuss now. At first, we have measured the possible cytotoxicity of ICG attached hybrid graphene oxide and for this purpose, ICG-bound hybrid graphene oxide attached G361 malignant melanoma cells were incubated for 12 hours without any NIR light. As shown in Figure 3D, our experimental data indicate no cell death even after 12 hours of incubation, which indicates that ICG-bound hybrid graphene oxide is not cytotoxic in the absence of external NIR light. On the other hand, as shown in Figure 3D, NIR light induced experimental data clearly show that 99% of cells were dead, when ICG-bound hybrid graphene oxide attached G361 malignant melanoma cells were irradiated with 785 nm light at 1 W/cm² power for 20 minutes. Bright-field inverted microscope images data as shown in Figure 3C, clearly show G361 malignant melanoma cells were deformed during the combined therapy process. The cell death following nanoplateform exposure to 785 nm NIR light could be due to numerous factors including ROS induced cancer cell death due to the presence of ICG and thermal disintegration by graphene oxide. Figure 3D also shows that

35

about 50 % cancer cell is dead when only ICG was used for the photodynamic therapy of G361 malignant melanoma cells using 785 nm light at 1 W/cm² power for 20 minutes. Next, to understand how the temperature varies during NIR radiation based combined therapy process, we have used a MikroShot Camera to measure thermal imaging at 1-minute intervals. Our thermal imaging experiments indicate that the temperature increased to about 40°C when ICG bound AGE aptamer attached hybrid graphene oxide with G361 malignant melanoma cells were exposed to 785 nm laser light at 1 W/cm² power for 20 minutes. We have also noted that the temperature increased to only 28°C for G361 malignant melanoma cells in the absence of hybrid magnetic graphene oxide under the same light exposure condition. All the above reported therapy data clearly indicate that malignant melanoma cell viability was much lower in the case of PDT & PTT combined therapy, than that by the individual ones. Our experimental data show that when the two treatments were combined under a single 785 nm NIR light irradiation, synergistic therapeutic effect are expected for the G361 malignant melanoma cells.

In ICG-bound AGE aptamer attached hybrid graphene oxide, ICG utilizes his ability to form reactive oxygen species in the presence of light to kill G361 malignant melanoma cells. As a result, the efficiency of photodynamic killing by hybrid graphene oxide is highly dependent on the formation of ROS capability by ICG. To understand the mechanism for the synergistic combined therapy to destroy G361 malignant melanoma cells, we have measured the cellular ROS formation during PDT and combined therapy process using singlet oxygen sensor green reagent (SOSG, Sigma). The fluorescence intensity was measured using the microplate reader with the excitation wavelength at 485 nm and the emission wavelength at 528 nm. As reported in Figure 3E, our experimental data clearly show the elevated ROS formation in the presence of AGE aptamer attached hybrid graphene oxide, which indicate that the photothermal effect of graphene oxide was able to enhance the formation of singlet oxygen, which improved photodynamic cancer cell killing efficiency. Due to the above fact, we observed synergistic therapeutic effect.

Conclusion

In conclusion, in this manuscript, we have reported the development of aptamer-conjugated hybrid graphene oxide which can deliver targeted separation, diagnostic and combined synergistic photothermal & photodynamic treatment of malignant melanoma cancer cells. We have found that the AGE-aptamer attached magnetic graphene oxide can be used for the ultra-sensitive and label-free detection of G361 malignant melanoma cells from infected blood sample. Excitation wavelength dependent photoluminescence imaging data indicate that aptamer-attached hybrid graphene can be used as multi-color luminescence platform for selective imaging of malignant melanoma cells. We have shown that in the absence of NIR light, no cytotoxicity has been observed from hybrid graphene oxide. Whereas, ICG-bound AGE aptamer attached hybrid graphene oxide can be used for 785 nm NIR light activated combined PTT & PDT therapy for G361 malignant melanoma cells. Reported experimental data indicate that synergistic therapeutic effect can be obtained using ICG-bound AGE aptamer attached hybrid graphene oxide, which indicates that the multimodal therapeutic material using ICG-bound hybrid graphene oxide may become a more effective system for malignant melanoma cancer therapy.

Though we are in a relatively early stage of development of aptamer attached hybrid graphene oxide based CTC separation, imaging and synergistic combined therapy of malignant melanoma, we believe that the reported assay can have enormous potential for real life applications, once it is optimized properly in clinical settings.

Acknowledgements

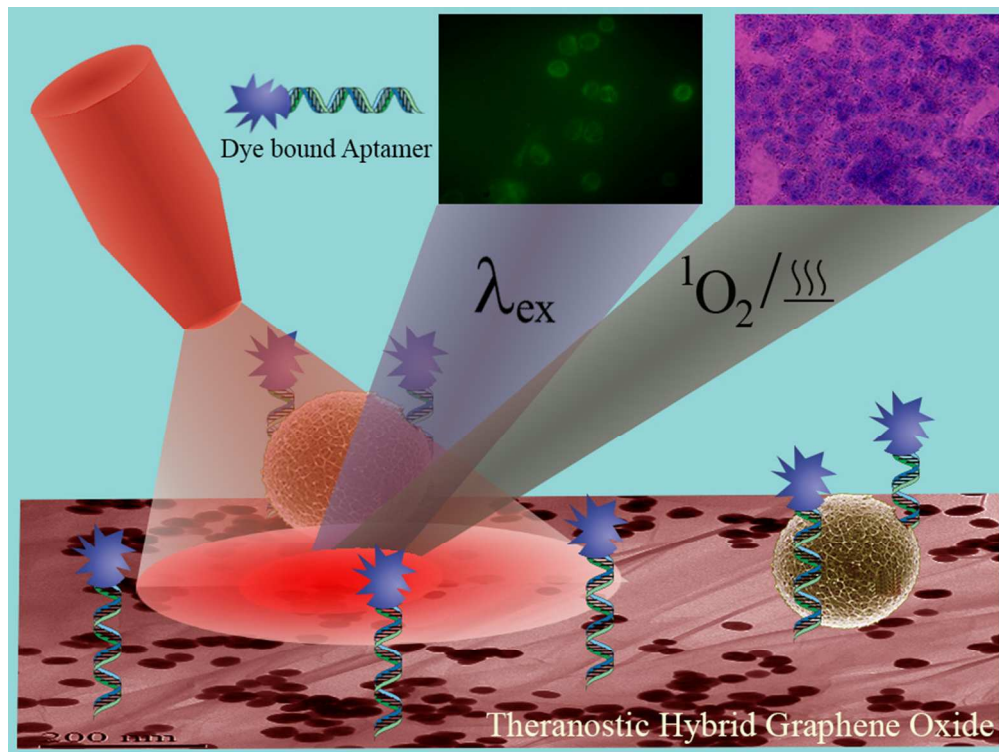
Dr Ray thanks NSF-PREM (grant ## DMR-1205194) and NSF-REU grant # 1156111 for generous funding.

Notes and References

1. www.cancer.org/aboutus/globalhealth, date of access 03/12/2014
2. www.cancer.org/cancer/skincancer-melanoma, date of access 03/12/2014
3. K. Pantel, R. H. Brakenhoff, B. Brandt, *Nat. Rev. Cancer* 2008, **8**, 329–340.
4. H. Lui, J. Zhao, D. McLean and H. Zeng, *Cancer Res.*, 2012, **72**, 2491–2500
5. A.; Ojima, M. Takanori, M. Sayaka, T. Masayoshi, I. Hiroyoshi Inoue, H. Yuichiro and Y. Sho-ichi, *Laboratory Investigation* 2014, **94**, 422–429.
6. S. David, Q. Zhang, W. Xuexi, P. He, Y. J. Zhu, J. Zhao, O. M. Rennert, and Y. A. Su, *Mol. Cancer Ther* 2009;**8**:1292–1304
7. E. C. Dreaden, A. M. Alkilany, X. Huang, C. J. Murphy and M. A. El-Sayed., *Chem. Soc. Rev.* 2012, **41**, 2740–2779.
8. E. I. Galanzha, E. V. Shashkov, T. Kelly, J. Kim, L. Yang, P. V. Zharov, *Nat. Nanotechnol.* **2009**, **4**, 855–860
9. Z. Fan, D. Senapati, A. K. Singh, P. C. Ray, *Mol. Pharmaceutics* 2013, **10**, 857–866.
10. Z. Fan, X. Dai, Y. Lu, E. Yu, N. Brahmabatt, NaTasha Carter, C. Tchouwou, A. K. Singh, Y. Jones, H. Yu, and P. C. Ray, *Mol. Pharmaceutics*, 2014, **11**, 1109–1116.
11. S. Lal, S. E. Clare, N. J. Halas, *Acc. Chem. Res.* 2008, **41**, 1842–1851
12. A. K. Singh, S. A. Khan, Z. Fan, T. Demeritte, D. Senapati, R. Kanchanapally and P. C. Ray, *J. Am. Chem. Soc.* 2012, **134**, 8662–8669.
13. S. R. Panikkanvalappil, M. A. Mackey, M. A.; El-Sayed, *J. Am. Chem. Soc.* 2013, **135**, 4815–4821.
14. X. H. Huang, I. H. El-Sayed, W. Qian and M. A. El-Sayed, *J. Am. Chem. Soc.*, 2006, **128**, 2115–2120
15. X. Dai; Z. Fan, Y. Lu, P. C. Ray, *ACS Applied Mater. Sci.* 2013, **5**, 11348–11354
16. Z. Fan, D. Senapati, S. A. Khan, A. K. Singh, A. Hamme, B. Yust, D. Sardar, P. C. Ray, *Chem. A. Eur. J.*, 2013, **19**, 2839–2847
17. K. Cheresch, D. A. Yang, H. M. Reisfeld, R. A. Disialoganglioside, *Cancer Res.*, 1987, **47**, 1098–1104.
18. R. Kanchanapally, Z. Fan, A. K. Singh, S. S. Sinha and P. C. Ray, *J. Mater. Chem. B*, 2014, **2**, 1934–1937
19. B. Tian, C. Wang, S. Zhang, L. Feng, Z. Liu, *ACS Nano* 2011, **5**, 7000–7009
20. J. T. Robinson, S. M. Tabakman, Y. Liang, H. Wang, H. S. Casalongue, D. Vinh and H. Dai, *J. Am. Chem. Soc.*, 2011, **133**, 6825–6831
21. M. Li, X. Yang, J. Ren, K. Qu and X. Qu, *Adv. Mater.*, 2012, **24**, 1722–1728
22. M.-C. Wu, A. R. Deokar, J.-H. Liao, P.-Y. Shih and Y.-C. Ling, *ACS Nano*, 2013, **7**, 1281–1290
23. Z. Fan, R. Kanchanapally, P. C. and Ray, *J. Phys. Chem. Lett.* 2013, **4**, 3813–3818
24. A. K. Geim, K. S. Novoselov, *Nat. Mater.* 2007, **6**, 183–191
25. W. Gao, B. L. Alemany, L. Ci, P. M. Ajayan, *Nat. Chem.* 2009, **1**, 403–408.
26. Y. Liang, Y. Li, H. Wang, H. Dai, *J. Am. Chem. Soc.*, 2013, **135**, 2013–2036
27. A. Sinitksii, J. M. Tour, *J. Am. Chem. Soc.* 2010, **132**, 14730–14732
28. I. V. Lightcap, and P. V. Kamat, *Acc. Chem. Res.*, 2013, **46**, 2235–2243

29. M. Z. Hossain, J. E. Johns, K. H. Bevan, J. H. Karmel, Y. T. Liang, S. Yoshimoto, K. Mukai, T. Koitaya, J. Yoshinobu, M. Kawai, *et. al. Nat. Chem.* 2012, **4**, 305–309
30. K. P. Loh, Q. Bao, G. Eda, & M. Chhowalla, *Nat. Chem.* 2010, **2**, 1015–1024.
31. J. Kim, L. J. Cote, F. Kim, & J. Huang, *J. Am. Chem. Soc.* 2010, **132**, 260.
32. S. K. Cushing, M. Li, F. Huang, and N. Wu, *ACS Nano*, 2014, **8**, 1002.
33. A. L. Exarhos, M. E. Turk, J. M. Kikkawa, *Nano Lett.* 2013, **13**, 344–348.
34. X. Zheng, D. Xing, F. Zhou, B. Wu and W. R. Chen, *Mol. Pharm.*, 2011, **8**, 447–456.
35. M. A. Yaseen, J. Yu, B. Jung, M. S. Wong, B. Anvari, *Mol. Pharmaceutics* 2009, **6**, 1321–1332
36. J. Yu, D. Javier, M. A. Yaseen, N. Nitin, R. Richards-Kortum, B. Anvari, M. S. Wong, *J. Am. Chem. Soc.* 2010, **132**, 1929–1938
37. J. Lin, S. Wang, P. Huang, Z. Wang, S. Chen, G. Niu, W. Li, J. He, D. Cui, G. Lu, X. Chen, Z. Nie, *ACS Nano* 2013, **7**, 5320–5329
38. Hummers, W. S.; Offeman, R. E. *J. Am. Chem. Soc.* 1958, **80**, 1339–1339.
39. Yoon, H. J.; Kim, T. H.; Zhang, Z.; Azizi, E.; Pham, T. M.; Paoletti, C.; Lin, J.; Ramnath, N.; Wicha, M. S.; Hayes, D. F. *et al. Nat. Nanotechnol.* 2013, **8**, 735–741
40. Fan, J.; Singh, A. K.; Sinha, S. S.; and Ray, P. C.;, *J. Mater. Chem. B*, 2014, **2**, 1934–1937.
41. Yin, S.; Wu, Y. L.; Hu, B.; Wang, Y.; Cai, P.; Tan, C. K.; Qi, D.; Zheng, L.; Leow, W. R.; Tan, N. S. *Adv. Mater. Interfaces* 2014, **1**, 1300043

30



254x190mm (96 x 96 DPI)